DMD Fast Forward. Published on December 8, 2014 as DOI: 10.1124/dmd.114.060061
This article has not been copyedited and formatted. The final version may differ from this version.

TITLE:

Absorption, metabolism and excretion of oral ^{14}C radiolabeled ibrutinib: An open-label, phase I, single-dose study in healthy men

Authors:

Ellen Scheers, Laurent Leclercq, Jan de Jong, Nini Bode, Marc Bockx, Aline Laenen, Filip Cuyckens , Donna Skee, Joe Murphy, Juthamas Sukbuntherng, Geert Mannens

Pharmacokinetics, Dynamics and Metabolism, Janssen R&D, Beerse, Belgium (E.S., L.L., M.B., A.L., F.C., G.M.);

Clinical Pharmacology, Janssen R&D, San Diego, CA, USA (J.D.J.);

Pre-Clinical Project Development, Janssen R&D, Beerse, Belgium (N.B.);

Clinical Pharmacology, Janssen R&D, Raritan, NJ, US (D.S., J.M.);

Pharmacyclics, Sunnyvale, CA, USA (J.S.);

Running title: Absorption, metabolism and excretion of ibrutinib

Corresponding author:

Geert Mannens

Senior Scientific Director & Fellow

Pharmacokinetics, Dynamics and Metabolism

Janssen R&D, Turnhoutseweg 30,

B-2340 Beerse, Belgium

Tel +32 14603745

Fax +32 14605110

Email: gmannens@its.jnj.com

Number of text pages: 31

Number of tables: 3

Number of figures: 5

Number of references: 11

Number of words:

Abstract: 250

Introduction: 284

Discussion: 1440

Abbreviations:

AE, adverse events; AUC_{24}, area under the concentration-time curve from time 0 to 24 h; AUC∞, AUC from time 0 to infinite time; $AUC_{last,}$ AUC from time 0 to time of the last quantifiable concentration; CL/F, total clearance; CLL, chronic lymphocytic leukemia; $CL_{R,}$ renal clearance; $C_{max,}$ maximum concentration; CV, coefficient of variation; CYP, cytochrome P450; ECG, Electrocardiogram; EOS, end-of-study; FDA, Food and Drug Administration; GI, gastrointestinal; LC-MS/MS, mass spectrometry/mass spectrometry; MCL, mantle cell lymphoma; NCI-CTCAE, National Cancer Institute - common terminology criteria for adverse events; SD, standard deviation; SDS, sodium dodecyl sulphate; SPE, solid phase extraction; t½, elimination half-life; $t_{last,}$ time to last quantifiable concentration; $t_{max,}$ time to reach C_{max}; UPLC, reversed phase ultra performance liquid chromatography; Vd/F, apparent volume of distribution based on the terminal phase

Abstract:

The absorption, metabolism, and excretion of ibrutinib were investigated in healthy men after administration of a single oral dose of 140 mg of ^{14}C-labeled ibrutinib. The mean (SD) cumulative excretion of radioactivity of the dose was 7.8 (1.4) % in urine and 80.6 (3.1) % in feces with <1% excreted as parent ibrutinib. Only oxidative metabolites and very limited parent compound were detected in feces, and this indicated that ibrutinib was completely absorbed from the GI tract. Metabolism occurred via three major pathways (hydroxylation of the phenyl (M35), opening of the piperidine (M25 and M34), and epoxidation of the ethylene on the acryloyl moiety with further hydrolysis to dihydrodiol (PCI-45227, M37). Additional metabolites were formed by combinations of the primary metabolic pathways or by further metabolism. In blood and plasma, a rapid initial decline in radioactivity was observed along with long terminal t1/2 for total radioactivity. Cmax and AUC for total radioactivity were higher in plasma compared with blood. The main circulating entities in blood and plasma were M21 (sulphate conjugate of a mono-oxidized metabolite on phenoxyphenyl), M25, M34, M37 (PCI-45227) and ibrutinib. At Cmax of radioactivity, 12% of total radioactivity was accounted for by covalent binding in human plasma. More than 50% of total plasma radioactivity was attributed to covalently bound material from 8 h onwards; as a result, covalent binding accounted for 38% and 51% of total radioactivity $AUC_{0\text{-}24h}$ and $AUC_{0\text{-}72h}$, respectively. No effect of CYP2D6 genotype was observed on ibrutinib metabolism. Ibrutinib was well-tolerated by healthy participants.

DMD Fast Forward. Published on December 8, 2014 as DOI: 10.1124/dmd.114.060061
This article has not been copyedited and formatted. The final version may differ from this version.

Introduction

Imbruvica™ (ibrutinib) is a first-in-class, potent, orally administered, covalently binding inhibitor of Bruton's tyrosine kinase (Btk) in B-cell malignancies, currently under development (Winer et al., 2012; Herman et al., 2011; Brown, 2013). The US Food and Drug Administration declared ibrutinib as a breakthrough therapy (February 2013) for the treatment of relapsed/refractory (R/R) mantle cell lymphoma (MCL) and gave approval for this indication in November 2013 (Wang et al., 2013). Recently (February 2014) FDA provided an accelerated approval for ibrutinib for chronic lymphocytic leukemia (CLL) in patients who had received at least 1 previous therapy (Byrd et al., 2013; O'Brien et al., 2014). Ibrutinib could change the paradigm for treatment of patients with MCL and CLL wherein intensive combination therapies are utilized.

Pharmacokinetic studies in rodents demonstrated that ibrutinib is rapidly absorbed following oral administration and first-pass metabolism may be a reason for low oral bioavailability (Honigberg et al., 2010). A mass balance study with racemic mixture of ^{14}C-ibrutinib (*R*-enantiomer) and ^{14}C-PCI-32769 (*S*-enantiomer) in rats indicated hepatic metabolism as a primary route of elimination. Also, *in vitro* studies had shown that ibrutinib is extensively metabolized primarily by CYP3A4/5 and to a lesser extent by CYP2D6 enzymes (Imbruvica™ Prescribing Information). Pharmacokinetic findings of studies in humans also showed rapid absorption and elimination of ibrutinib (Advani et al., 2013). Also, ibrutinib does not have toxic effects on normal T cells, which distinguishes it from most regimens used for CLL (Byrd et al., 2013).

The objective of this study was to investigate the absorption, metabolic pathways, and excretion routes of ibrutinib in healthy men after administration of a single oral dose of 140 mg (5 mg/mL

solution) of unlabeled ibrutinib admixed with ^{14}C-ibrutinib. Additionally, safety was also evaluated.

Materials and Methods

Study participants

Healthy, nonsmoking men, 30 to 55 years old (inclusive) with a body mass index between 18 and 30 kg/m² (inclusive) and body weight ≥ 50 kg were enrolled in the study. In order to assess the relative contribution of CYP3A4 versus CYP2D6 metabolism, 2 CYP2D6-poor metabolizers (evident from genotype analysis at screening) were enrolled. Various 2D6 genotypes were tested for each participant. Participant 1 and 2 expressed *5/*5 and *4/*4, respectively. Based on Covance's Affymetrix software, the phenotypes were predicted to be poor metabolizers. This was done prospectively as part of the screening process.

Samples were analyzed similarly for 3A4 and 3A5. All subjects had predicted 3A4 phenotypes as extensive metabolizers and all subjects had predicted 3A5 phenotypes as poor metabolizers.

Participants with irregular bowel movements or clinically significant abnormal values for hematology, coagulation and platelet function were excluded from the study.

The Independent Ethics Committee approved the protocol and the study was conducted in accordance with the ethical principles that have their origin in the Declaration of Helsinki and that are consistent with Good Clinical Practices and applicable regulatory requirements. All patients provided a written informed consent before enrollment.

Study design

This study was a phase 1, open-label, single-center, single-dose study conducted from August 2012 to September 2012. The study consisted of a screening (day -28 to day -2), baseline (day -2 to day -1; admission to study unit on day -2), open-label (15 days), end-of-study (EOS) (up to day 15), and follow-up phases (30 days after EOS).

Whole blood, plasma, urine, and feces were collected for a minimum of 7 days after dosing (i.e., until day 8), and possibly for up to 7 more days (i.e., up to day 15) if radioactivity in the excreta (i.e. 24-h urine and feces) on either day 6 or 7 accounted for ≥2% of the total administered dose or if <7 fecal samples were obtained by day 8. The occurrence of adverse events (AEs) was monitored throughout the study. A telephonic follow-up was conducted 30 days after discharge from the study unit to collect information on any AEs.

Study medication

An oral solution of 14C-ibrutinib targeting 5 mg base eq/mL, a radioactivity concentration of 52.9 kBq/mL, and a specific radioactivity of 10.6 kBq/mg base-eq was prepared by dilution of high specific activity 14C-ibrutinib with a 30% hydroxypropyl-β-cyclodextrin formulation of unlabeled ibrutinib. The 14C label is located on the carbonyl moiety.

On day 1, following an overnight fast, each of the 6 participants received a single oral solution dose of 140 mg ibrutinib containing 1480 kBq (40 μCi) of 14C-ibrutinib. The radiation burden received by a human subject after an orally administered radioactivity of 1480 kBq (or 40 μCi) associated with 14C-ibrutinib has been calculated, using formulae and data recommended by the International Commission of Radiation Units and Measurements (Recommendations of the International Commission on Radiological Protection. ICRP Publication 103. March 2007). Evaluations of the absorbed radiation in single organs were based on data from a quantitative

whole-body autoradiography (QWBA) study measuring the tissue distribution of the total radioactivity in male Lister Hooded rats after administration of a single oral gavage dose of a solution of 14C-ibrutinib at 10 mg/kg. The calculations of the radiation dose to the gastro-intestinal tract and the bladders (stomach, gall bladder, small intestine, upper and lower large intestine and urinary bladder) were based on the excretion profile in rats, and have been made assuming that their exposure results entirely from radioactive material in their contents, and that the mean residence times and throughput of those contents have standard values. The weighted dose-equivalents of the ICRP recommended organs have been summed to obtain the committed effective dose to the whole body of man, after oral administration of radiolabelled ibrutinib. Oral administration of 1480 kBq (or 40 µCi) 14C- ibrutinib was calculated to result in a total radiation burden of 916 µSv. An effective dose (total body) between 100 and 1 000 µSv is categorised as a category IIa project (a minor level of risk, covering doses to the public from controlled sources) (Radiological Protection in Biomedical Research. ICRP Publication 62. November 1992). The vial used for drug administration was rinsed 3 times with plain noncarbonated water and the participants consumed the rinsing fluids along with additional plain noncarbonated water (240 mL).

Pharmacokinetic evaluations

Sample collection

Blood samples were collected for determination of ibrutinib and PCI-45227 concentrations in blood and plasma, and total radioactivity predose and at 0.5, 1, 1.5, 2, 3, 4, 6, 8, 12, 16, 24, 48, and 72 h post-dose. Plasma protein binding was evaluated using predose samples. Covalent binding of total radioactivity to plasma proteins was evaluated in pooled human samples

collected at 1, 2, 4, 8, 24 and 72 h post-dose. The plasma pellets, generated during the preparation of plasma (for metabolite identification) were used to further investigate possible covalent binding of ibrutinib and/or metabolites to proteins with different extraction steps. Plasma pellets were redissolved in 1% SDS (sodium dodecyl sulphate); proteins were homogenized in a mixture of acetonitrile/isopropyl alcohol/0.02% formic acid (6/3/1 v/v/v) and precipitated following centrifugation. Resuspension of the resulting pellet in the same organic solvent mixture and centrifugation was repeated twice. Radioactivity in the different supernatant fractions and in the final pellet (redissolved in 4 M urea + 1% SDS) was determined by liquid scintillation counting. Urine and feces (analyzed per stool) were collected pre-dose and at 0-2, 2-4, 4-8, 8-24, 24-48, 48-72, 72-96, 96-120, 120-144, and 144-168 h post-dose. However, for metabolic profiling, blood and plasma, were collected predose and at 1, 2, 4, 8, 24, and 72 h post-dose. For metabolic profiling of urine and feces, a selection of samples was made. Baseline glomerular filtration rate was calculated based on 24-h urine collection and serum creatinine measurement on day -1.

Bioanalytical procedures

Plasma samples were analyzed to determine concentrations of ibrutinib and PCI-45227 using a validated liquid chromatography coupled to mass spectrometry/mass spectrometry (LC-MS/MS) method. Blood and urine samples were analyzed to determine concentrations of ibrutinib and PCI-45227 using qualified assays (manuscript in development). Total radioactivity (^{14}C) was measured in blood, plasma, urine, and feces using liquid scintillation counting in a Packard Tri-Carb 2900 TR liquid scintillation spectrometer. Blood and feces residues were combusted in a Packard Sample Oxidizer 307 prior to liquid scintillation counting. Concentrations of ^{14}C-ibrutinib and ^{14}C-metabolites were measured in blood, plasma, urine, and feces. Metabolic

profiling was performed on selected blood, plasma, urine, and feces samples using reversed phase Ultra Performance Liquid Chromatography (UPLC) with on-line (Scintillation solvent : Ultima-Flo-M (^{14}C-label), 3.8 mL/min using switching valve) or off-line radioactivity detection (TopCount/Deepwell Lumaplate combination, Perkin Elmer) and on-line mass spectrometry (MS or MSMS) data acquisition for metabolite identification (Supplementary data). The UPLC system was Acquity Binary Solvent Manager (Waters) and a Waters 2777 CTC_Pal injector equipped with a UV detector (Acquity PDA); the UPLC column was an Interchim Uptisphere Strategy 100Å C18-2, 2.2 µm, 2 x (150 mm x 3.0 mm (id)) (kept at 60°C, mobile phase flow rate: 0.8 mL/min). The mass spectrometer (QTOF Ultima, Waters) was equipped with a dual electrospray ionization probe and calibrated with a sodium formate solution delivered through the sample spray. The QTOF data (MS, MSMS) was acquired in the centroid mode with a variable scan time (0.5 – 1.0 s). All data were processed using Masslynx mass spectrometry software (Waters Corporation).

Sample preparation

Feces

Pooled feces homogenates were extracted using a 3-step extraction procedure with acetonitrile/isopropyl alcohol/0.02% formic acid (6/3/1) as extraction solvent. Dried down fecal extracts were reconstituted in DMSO (1000 µL) prior to injection on UPLC (750 µL) with solid phase extraction (SPE) (Interchim Uptisphere Strategy 100Å C18-2, 2.2 µm, 2 x (150 mm x 3.0 mm(id)) and online counting.

Urine

DMD Fast Forward. Published on December 8, 2014 as DOI: 10.1124/dmd.114.060061
This article has not been copyedited and formatted. The final version may differ from this version.

Urine was thawed at room temperature and centrifuged. After centrifugation, 28.0 or 36.0 mL of the supernatant was injected for UPLC analysis using online SPE (Interchim Uptisphere Strategy 100Å C18-2, 2.2 µm, 2 x (150 mm x 3.0 mm(id)) and on-line detection of total radioactivity.

Blood

Blood samples were thawed at room temperature. Blood (24 mL pools at 1, 2, 4, 8, 24 and 72h) was precipitated with acetonitrile (1/1, v/v). After vortexing and centrifugation, approximately 28.8 to 30.6 mL of the supernatant was injected for UPLC analysis using online SPE (Interchim Uptisphere Strategy 100Å C18-2, 2.2 µm, 2 x (150 mm x 3.0 mm(id)) and off-line counting of total radioactivity using a TopCount/Deepwell Lumaplate combination (Perkin Elmer).

Plasma

Protein precipitation for plasma sample preparation was performed using acetonitrile (1/1, v/v). Individual 8 ml samples were analyzed at 1h, 2h and 4h, and three 24-mL pools across participants were made for the 8, 24 and 72h plasma samples. After vortexing and centrifugation, total radioactivity was determined in a subsample using liquid scintillation counting in order to determine the recovery of total radioactivity. The supernatant was injected for UPLC analysis using online SPE (Interchim Uptisphere Strategy 100Å C18-2, 2.2 µm, 2 x (150 mm x 3.0 mm(id)) and off-line counting of total radioactivity using a TopCount/Deepwell Lumaplate combination (Perkin Elmer).

Pharmacokinetic parameters

The following pharmacokinetic parameters were estimated from total radioactivity or unchanged drug and metabolite concentrations in whole blood, plasma, urine, and feces samples: maximum

DMD Fast Forward. Published on December 8, 2014 as DOI: 10.1124/dmd.114.060061
This article has not been copyedited and formatted. The final version may differ from this version.

concentration (C_{max}); time to reach C_{max} (t_{max}); area under the concentration-time curve from time 0 to 24 h (AUC_{24}); AUC from time 0 to time of the last quantifiable concentration (AUC_{last}); AUC from time 0 to infinite time (AUC_{∞}), calculated as the sum of AUC_{last} and $C_{last/\lambda z}$, in which C_{last} is the last observed quantifiable concentration; elimination half-life ($t_{½}$) time to last quantifiable concentration (t_{last}); apparent volume of distribution based on the terminal phase (Vd/F), calculated as $D/(\lambda_{z*}AUC_{\infty})$; renal clearance ($CL_R$) of drug, calculated as Ae_{∞}/AUC_{∞}; total clearance (CL/F) of drug after extravascular administration, calculated as D/AUC_{∞}.

Pharmacogenomic evaluations

Blood samples (10 mL) of participants were collected for pharmacogenomics evaluation at screening to determine their CYP2D6 metabolizer status by genotyping. The DNA samples from enrolled participants were also analyzed for CYP3A4 and CYP3A5 status.

Safety evaluations

Safety and tolerability were evaluated throughout the study and consisted of assessment of AEs from the time of obtaining informed consent to EOS or early withdrawal assessment. Scheduled safety assessments of 12-lead ECG, physical examination, vital signs, and clinical laboratory investigations (hematology, serum chemistry, and urinalysis) occurred before the administration of study drug and at the EOS assessment (after collection of the final fecal sample). The AE severity was graded according to the National Cancer Institute - Common Terminology Criteria for Adverse Events (NCI-CTCAE) grading system version 4.03.

Statistical methods

Sample size

DMD Fast Forward. Published on December 8, 2014 as DOI: 10.1124/dmd.114.060061
This article has not been copyedited and formatted. The final version may differ from this version.

The sample size of 6 patients with a minimum of 4 to complete the study was considered adequate to generate meaningful descriptive measures of the pharmacokinetics (absorption, metabolism, and excretion) of ibrutinib.

Analysis sets

All enrolled participants completed the study and were included in the pharmacokinetic and safety analysis population.

Analysis

Individual and mean blood and plasma ibrutinib and PCI-45227 concentration-time profiles were plotted. Blood and plasma concentration data at each time point were summarized with mean, median, geometric mean, minimum, maximum, standard deviation (SD) and coefficient of variation (CV%). All estimated pharmacokinetic parameters of ibrutinib and PCI-45227 were summarized with mean, median, geometric mean, minimum value, maximum value, SD, and CV%. Individual genotype status for CYP3A4/5 and CYP2D6 were listed.

Results

Study participants

All participants (n=6) were white healthy men with median (range) age of 51 years (35 to 55 years); baseline weight of 82.5 (61.7 to 87.3) kg; height of 176 (163 to 179) cm and baseline body mass index 25.8 (22.7 to 28.9) kg/m^2.

Pharmacokinetic results

Drug concentration measurements and total radioactivity in whole blood and plasma

DMD Fast Forward. Published on December 8, 2014 as DOI: 10.1124/dmd.114.060061
This article has not been copyedited and formatted. The final version may differ from this version.

After dosing, mean concentration-time profiles in blood and plasma were similar for ibrutinib and for PCI-45227 (Figure 1). Mean ibrutinib and PCI-45227 concentrations were lower than the total radioactivity in both blood and plasma (Figure 2). All participants had measurable blood concentrations of total radioactivity for 4 h after dosing. In total 5 out of 6 participants had measurable radioactivity for 8 h and only 1 participant had measurable radioactivity at 24 h. Concentrations of total radioactivity in plasma were measurable for all participants for 72 h after dosing. The fact the blood concentrations could not be measured at later time point was due to a higher limit of quantification for blood as compared to plasma. In blood and plasma, a rapid initial decline in radioactivity was observed along with long terminal half-life for total radioactivity. Most of the total radioactivity was associated with plasma rather than the cellular components of whole blood (Figure 2). The mean blood to plasma concentration ratio of total radioactivity was approximately 0.7.

Ibrutinib and PCI-45227 in urine

Total 5 of the 6 participants, had measurable but very low levels of ibrutinib in urine from 0 to 2 h after dosing and 1 participant also between 2 and 4 h. The mean total amount excreted was 0.000176% of the dose. PCI-45227 was measurable in urine in all participants through 72 h. after dosing and in 2/6 participants through 96 h. The mean total amount (ibrutinib and PCI-45227) excreted was 0.12% of the dose.

Total radioactivity in urine and feces

The mean (SD) cumulative excretion of radioactivity in urine was 7.8 (1.4) % of the dose and majority of the radioactivity was excreted within 24 h after dosing. In feces, mean (SD) cumulative excretion of radioactivity accounted for 80.6 (3.1) % of the dose and majority of the

radioactivity was excreted within 48 h after dosing (Figure 3A-3D). Total excretion in the 0-168 h period post dose amounted to 88.5 (4.3) %.

Pharmacokinetic Parameters

The pharmacokinetic parameters of ibrutinib and PCI-45227 were similar for blood and plasma (Table 1). Total radioactivity C_{max} and AUC in both plasma and blood were several-fold higher than that for ibrutinib and PCI-45227. Mean (SD) unbound ibrutinib was 2.3 (0.3) % or 97.7 % bound. Creatinine clearance ranged from 112 mL/min to 159 mL/min and confirmed that participants had normal renal function.

Metabolite Identification

Three main metabolic pathways for ibrutinib were distinguished based on the nature of the identified metabolites: hydroxylation of the phenyl (M35), opening of the piperidine with further reduction to a primary alcohol (M34) or oxidation to a carboxylic acid (M25), and epoxidation of the ethylene on the acryloyl moiety followed by hydrolysis to a dihydrodiol (M37, also referred to as PCI-45227). Most remaining metabolites were formed by combinations or by further secondary metabolism of these main metabolites (Figure 4).

In feces, 12 metabolites and unchanged drug were identified as the main entities (40% of the administered dose) and ibrutinib was present in minor quantity (0.77% of the administered dose). The main metabolites identified in feces were M20 (oxidation product of M25), M25 and M34, each between 5-10% of the dose. Of note, M34 appeared to co-elute with other metabolites in urine and feces, but was the main entity under the radioactive peak using MS detection.

DMD Fast Forward. Published on December 8, 2014 as DOI: 10.1124/dmd.114.060061
This article has not been copyedited and formatted. The final version may differ from this version.

The observed metabolites in blood and feces were very similar (Figure 5). In urine, the majority of the observed metabolites were assigned to the piperidine ring-opening metabolic pathway (3.84% of the administered dose). Table 2 provides an overview of the identified metabolites.

As metabolites were generally below the quantification limit of the radio-detector, metabolite profiles in blood and plasma could only be qualitatively compared, and are found to be similar. The main circulating entities in blood and plasma were M21 (sulphate conjugate of a mono-oxidized metabolite on the phenoxyphenyl), M25, M34, M37 and unchanged drug. These metabolites could be observed predominantly at 1 h post oral administration and rapidly eliminated through 4 h post-dose, except for M37, which was still detectable at 24 h post oral administration at 140 mg. Small amounts of M39 and M40 (both addition of one oxygen on the piperidine ring) were also detected in blood and plasma. Minor unlabeled metabolites were observed as well. M23 (unlabeled metabolite resulting from amide hydrolysis) and downstream metabolites M30 (+O-2H), M1 (sulphate of mono-oxidized M23) and M4 (glucuronide of mono-oxidized M23) were detected with mass spectrometry. In plasma M23, M30, M1 and M4 were observed, M1 was not observed in blood. The abundance of these unlabeled metabolites in blood (based on MS-response) was comparable to the abundance in plasma.

The time-course of covalently bound radioactivity in plasma was very flat with an apparent maximum at 8 h post-dose while the peak of total radioactivity in plasma (covalently and non-covalently bound) was observed at 1 h post-dose. Total 6-fold decline in total plasma radioactivity and slight decrease in covalently bound radioactivity was observed from peak to 24 h post-dose, with apparent long half-life confirmed based on the 72h time point. Based on a comparison of C_{max} values, at Cmax of radioactivity, 12% of total radioactivity was accounted

DMD Fast Forward. Published on December 8, 2014 as DOI: 10.1124/dmd.114.060061
This article has not been copyedited and formatted. The final version may differ from this version.

for by covalent binding in human plasma. Covalent binding accounted for 38% and 51% of total radioactivity AUC0-24h and AUC0-72h, respectively (Table 3).

As part of an in vitro plasma protein binding estimation, radiolabelled ibrutinib was spiked to human plasma at 500 ng/mL and covalent binding was assessed at various time points. Covalent binding gradually increased from 7.3% at 1 h to 24.9% at 8 h. Also an experiment assessing the covalent binding of ibrutinib to human plasma proteins was conducted at various concentrations (50, 500 and 1000 ng/mL) up to 30 minutes and did not highlight a concentration dependency of the covalent binding; at 30 min covalent binding averaged about 3%. A covalent binding experiment using purified human plasma proteins (α1 AGP and human serum albumin) and ibrutinib at 150 ng/mL showed that ibrutinib was mainly binding covalently to human serum albumin (10.2%) and minimally to α1 AGP (0.4-0.6%).

Pharmacogenomics

No difference in unchanged ibrutinib exposure (C_{max} and AUC) was observed between CYP2D6 poor metabolizers (n=2) and extensive metabolizers (n=4). PCI-45227 exposure (C_{max} and AUC) for one of the CYP2D6-poor metabolizers was approximately 40% higher than the median values for all other participants.

Safety

Two out of 6 participants in the safety analysis set experienced at least one AE. The reported AEs were abdominal pain, diarrhea, headache, and skin irritation with grade 1 or grade 2 severities and reported one time. No clinically relevant changes were observed in physical examination, clinical laboratory analyses, vital signs measurements, and ECGs.

Discussion

In this open-label phase 1 pharmacokinetic study, absorption, metabolic pathways, and route of excretion of orally administered radiolabeled ibrutinib were studied. Minimal excretion of unchanged ibrutinib, high levels of oxidative metabolites formed due to liver and gut metabolism and lack of reduction products in feces suggests complete absorption of ibrutinib from the GI tract. This study also supports the non-clinical data suggesting first-pass metabolism is the reason for low bioavailability of orally administered ibrutinib rather than poor absorption (Imbruvica™ Prescribing Information). Also, bioavailability is in line with other studies in healthy participants who were administered ibrutinib in a 40- or 140-mg capsule formulation (de Jong et al., 2014).

The pharmacokinetic parameters of ibrutinib and its dihydrodiol metabolite PCI-45227 were similar for blood and plasma. Higher plasma C_{max} and AUC for total radioactivity may be attributed to measurable concentration for longer time period in plasma (up to 72 h) as compared with blood (up to 8 h), due to the more sensitive plasma assay. Shorter mean half-life of ibrutinib as compared with PCI-45227 was not consistent with previous clinical studies (Imbruvica™ Prescribing Information). However, the estimate of ibrutinib half-life may have been limited by absence of measurable ibrutinib concentrations after 16 h. Also, longer radioactivity half-life in plasma as compared with blood may be due to fewer time points in the elimination phase.

Ibrutinib was extensively metabolized after a single dose of ^{14}C-ibrutinib with three main primary metabolic clearance pathways hydroxylation of the phenyl, opening of the piperidine and epoxidation of the ethylene on the acryloyl moiety with further hydrolysis to a dihydrodiol. Most of the ibrutinib metabolites (>95%) were oxidative in nature. Non-oxidative metabolites (<5%) were derived from glutathione addition to the acryloyl C=C. Other phase II metabolites

were minor and secondary to phase I (mostly sulphates of hydroxy- metabolites (<5% of dose). Direct sulfates or glucuronides of the parent were not observed. Metabolism at the acryloyl C=C resulted in mostly dihydrodiol formation which was consistent with *in vitro* studies and accounted for a relatively small proportion of the observed metabolites.

This study also characterized the ex-vivo plasma protein binding of ibrutinib in man which is consistent with the results obtained from *in vitro* studies. Slight decrease in covalently bound radioactivity from peak to 24 h post-dose suggested a slower process of protein turnover to clear covalently bound radioactivity from the circulation. The nature of the covalently bound radioactivity (parent vs metabolite) has not been investigated at this stage. Overall, the observation of significant covalent binding to plasma proteins is not unexpected as ibrutinib is by nature a covalent binder due to the presence of the Michael acceptor acryloyl moiety, which is also preserved in most of the observed metabolites.

When comparing total plasma radioactivity and covalently bound plasma radioactivity in the current human mass balance study at 1h, as close as possible to C_{max} (0.5 h), covalently bound plasma radioactivity (47 ng-eq/mL) represented around 8.5% of total plasma radioactivity (549 ng-eq/mL). However, the liver extraction ratio of ibrutinib is known to be high, which will lead to much higher ibrutinib concentrations in the portal vein as compared to the systemic circulation. Considering 92% liver extraction, the ibrutinib C_{max} of 37.1 ng/mL implies a portal vein concentration of around 464 ng/mL. Assuming a 30 min time window available for covalent binding in the portal vein based on a t_{max} of around 0.5 h in the mass balance study, 3% or about 14 ng-eq/mL would be covalently bound, which is around 30% of the observed 1-h post-dose level of 47 ng-eq/mL.

DMD Fast Forward. Published on December 8, 2014 as DOI: 10.1124/dmd.114.060061
This article has not been copyedited and formatted. The final version may differ from this version.

Covalent binding of radioactivity to the cellular fraction of blood was not assessed in this clinical study, but was assessed in rat and dog following oral dosing of 14C-labelled Ibrutinib. The in vivo radioactive studies in these animal species show a lot of similarities with the human study. In rat and dog, the time course of total radioactivity observed in blood and plasma was comparable to human (rapid initial decline followed by a long terminal half- life), with also an important contribution of circulating metabolites to the total radioactivity.

The blood to plasma ratio of total radioactivity was consistently lower than 1, similar to human (around 0.7 in dog up to 48h post dose, around 0.75 in rat, increasing to 1 or above at the later time points (24-48h)). Similarly to human plasma, the relative importance of covalent binding versus total radioactivity increased as a function of time post-dose, with covalent binding accounting for the majority of circulating radioactivity (both in plasma and blood) at the later time points, in line with the long terminal half-life.

In both rat and dog, the contribution of covalent binding to total radioactivity was higher for cellular components of blood than for plasma: covalent binding accounted for 30-40 % of total plasma radioactivity (AUC0-48h), in line with human, and for 60-70 % of total radioactivity in cellular components of blood (AUC0-48h). In the rat, at 1h post dose (close to Tmax), covalent binding in blood cellular components accounted for around 20% of total radioactivity in these cellular components, with a total blood radioactivity ranging between 694 (males) - 888 (females) ng-eq/mL. When spiking 440 ng-eq/mL Ibrutinib to blank rat blood and following incubation at 37°C for 1h, covalent binding in blood cellular components accounted for maximum 7 % of total radioactivity. As a result, and in line with the above reasoning for human plasma, it is not expected that the circulating levels of parent ibrutinib post liver can generate the

observed amount of covalent binding in blood cellular components; the observed covalent binding most probably results from high levels of unchanged drug in the portal vein (Ibrutinib also shows a high liver extraction ratio in rat and dog) with possible additional contribution of metabolites.

In conclusion, it is likely that the observed covalent binding in plasma can be attributed to ibrutinib for a significant part (around 30% as estimated upper limit), with albumin as the main target protein, and ibrutinib covalent binding occurring mainly pre-systemically. The remainder of the covalent binding in plasma can be attributed to ibrutinib metabolites (logically those bearing the acryloyl moiety intact), which can be formed via first pass gut or liver metabolism. Based on the structural similarity of metabolites with parent ibrutinib (except for the fact that some metabolites bear a ring-opened piperidine moiety), albumin would appear as a logical target protein for covalent binding of ibrutinib metabolites as well.

Small percentage of radioactivity recovered and negligible amount of unchanged drug present in urine suggested renal excretion to be a minor elimination pathway. Poor and extensive CYP2D6 metabolizers did not show apparent differences in ibrutinib pharmacokinetics and metabolism, which was consistent with the results from an *in vitro* study. The identification of cytochrome P450 isozymes responsible for the metabolism of ibrutinib was evaluated in vitro using recombinant CYP450 expressing different isozymes and human liver microsomes in the presence of CYP450 specific chemical inhibitors. CYP3A4/5 were identified to be the major human microsomal enzymes responsible for the metabolism of ibrutinib with no apparent involvement of CYP1A, CYP2B6, CYP2C8, CYP2C9, CYP2C19 or CYP2D6. Using the selective mechanism-based CYP3A4 inhibitor CYP3cide and comparing the metabolism of ibrutinib in

DMD Fast Forward. Published on December 8, 2014 as DOI: 10.1124/dmd.114.060061
This article has not been copyedited and formatted. The final version may differ from this version.

selected lots of human liver microsomes with functional or low to null CYP3A5 activity, the relative contribution of CYP3A5 of the overall metabolism of ibrutinib was estimated to be low (<20%).

Excretion profiles in poor and extensive metabolizers were highly comparable, no difference in the levels of any of the metabolites was detected between poor and extensive metabolizers. In plasma multiple metabolites were observed both in poor and extensive metabolizers. Next to unchanged drug, other major metabolites are circulating. There is no indication that one of the metabolites is more predominant in extensive metabolizers in comparison to poor metabolizers. There is no indication that the poor metabolizers are different from the extensive metabolizers with regards to excretion pathways and/or metabolism. No notable safety findings were reported during the study.

In summary, this study demonstrated that a single oral dose of 140 mg ibrutinib was completely absorbed from the GI tract followed by oxidative metabolism with three major pathways and minimal renal excretion. The C_{max} and AUC for total radioactivity were higher in plasma compared with blood. Ibrutinib and PCI-45227 each constituted less than 10% of the total circulating radioactivity. Approximately 12% of total radioactivity was accounted for by covalent binding in human plasma based on C_{max}, covalent binding accounted for 38% and 51% of total radioactivity $AUC_{0\text{-}24h}$ and $AUC_{0\text{-}72h}$, respectively. No apparent effect of poor and extensive CYP2D6 metabolizers was observed on pharmacokinetics and metabolism of ibrutinib. Also, ibrutinib was well-tolerated by healthy participants.

Acknowledgements:

The authors thank Rishabh Pandey (SIRO Clinpharm Pvt. Ltd.) for providing writing assistance and Dr. Namit Ghildyal (Janssen Research & Development, LLC) for additional editorial assistance. Our thanks also go to Prof. Dr. H. Thierens (State University of Ghent, Belgium) for evaluation of the radiation exposure and to the licensed radiopharmacist Prof. Dr. F. De Vos (State University of Ghent, Belgium). The authors also thank the study participants, without whom this study would not have been accomplished.

Author contributions:

Participated in research design: Scheers, Leclercq, de Jong, Bode, Bockx, Laenen, Cuyckens, Skee, Murphy, Sukbuntherng and Mannens

Performed data interpretation: Scheers, Leclercq, de Jong, Bode, Bockx, Laenen, Cuyckens, Skee, Murphy, Sukbuntherng and Mannens

Contributed to the writing of the manuscript: Scheers, Leclercq, de Jong, Bode, Bockx, Laenen, Cuyckens, Skee, Murphy, Sukbuntherng and Mannens

Conducted experiments: Skee, de Jong, Murphy, Cuyckens, Scheers, Laenen and Bockx

References

Advani RH, Buggy JJ, Sharman JP, Smith SM, Boyd TE, Grant B, Kolibaba KS, Furman RR, Rodriguez S, Chang BY, Sukbuntherng J, Izumi R, Hamdy A, Hedrick E, and Fowler NH (2013) Bruton tyrosine kinase inhibitor ibrutinib (PCI-32765) has significant activity in patients with relapsed/refractory B-cell malignancies. *J Clin Oncol* **31**(1):88-94.

Brown JR (2014) Ibrutinib in chronic lymphocytic leukemia and B cell malignancies. *Leuk Lymphoma* **55**:263–269.

Byrd JC, Fuman RR, Coutre, SE, Flinn IW, Burger JA, Blum KA, Grant B, Sharman JP, Coleman M, Wierda WG, Jones JA, Zhao W, Heerema NA, Johnson AJ, Sukbuntherng J, Chang BY, Clow F, Hedrick E, Buggy JJ, James DF, and O'Brien S (2013) Targeting BTK with ibrutinib in relapsed chronic lymphocytic leukemia. *New Engl J Med* **369**:32-42.

De Jong J, Skee D, Murphy J, Sukbuntherng J, Hellemans P, Smit H, de Vries R, Jiao J, and Mannaert E (2014) Effect of CYP3A perpetrators on ibrutinib exposure in normal healthy subjects. *Clinical Pharmacology & Therapeutics* **95**:S17-S56.

Herman SE, Gordon AL, Hertlein E, Ramanunni A, Zhang X, Jaglowski S, Flynn J, Jones J, Blum KA, Buggy JJ, Hamdy A, Johnson AJ and Byrd JC (2011) Bruton tyrosine kinase represents a promising therapeutic target for treatment of chronic lymphocytic leukemia and is effectively targeted by PCI-32765. *Blood* **117**(23):6287-6296.

Honigberg LA, Smith AM, Sirisawad M, Verner E, Loury D, Chang B, Li S, Pan Z, Thamm DH, Miller RA, and Buggy JJ (2010) The Bruton tyrosine kinase inhibitor PCI-32765 blocks B-cell

activation and is efficacious in models of autoimmune disease and B-cell malignancy. *Proc Natl Acad Sci U S A* **107**:13075-13080.

Imbruvica™ Prescribing Information. Reference ID: 3395788. http://www.accessdata.fda.gov/drugsatfda_docs/label/2013/205552lbl.pdf

O'Brien S, Furman RR, Coutre SE, Sharman JP, Burger JA, Blum KA, Grant B, Richards DA, Coleman M, Wierda WG, Jones JA, Zhao W, Heerema NA, Johnson AJ, Izumi R, Hamdy A, Chang BY, Graef T, Clow F, Buggy JJ, James DF, and Byrd JC (2014) Ibrutinib as initial therapy for elderly patients with chronic lymphocytic leukaemia or small lymphocytic lymphoma: an open-label, multicentre, phase 1b/2 trial. *Lancet Oncol* **15**(1):48-58.

Radiological Protection in Biomedical Research (1992) ICRP Publication 62. Ann ICRP 22 (3).

Recommendations of the International Commission on Radiological Protection (2007) ICRP publication 103. Ann ICRP 37(2-4):1-332.

Wang ML, Rule S, Martin P, Goy A, Auer R, Kahl BS, Jurczak W, Advani RH, Romaguera JE, Williams ME, Barrientos JC, Chmielowska E, Radford J, Stilgenbauer S, Dreyling M, Jedrzejczak WW, Johnson P, Spurgeon SE, Li L, Zhang L, Newberry K, Ou Z, Cheng N, Fang B, McGreivy J, Clow F, Buggy JJ, Chang BY, Beaupre DM, Kunkel LA and Blum KA (2013) Targeting BTK with ibrutinib in relapsed or refractory mantle-cell lymphoma. *N Engl J Med* **369**(6):507-16.

Winer ES, Ingham RR and Castillo JJ (2012) PCI-32765: a novel Bruton's tyrosine kinase inhibitor for the treatment of lymphoid malignancies. *Expert Opin Investig Drugs*. **21**(3):355-61.

Footnotes

Drs. Mannens, Leclercq, Bode, Cuyckens and Mrs. Scheers, Laenen and Mr. Bockx are employees of Janssen R&D, Belgium. Dr. de Jong, Ms. Skee, and Mr. Murphy are employees of Janssen R&D, LLC, USA. The Janssen companies are Johnson & Johnson companies. Drs. Mannens, Leclercq, Bode, Cuyckens, de Jong and Mr. Murphy hold stocks in Johnson & Johnson. Dr. Sukbuntherng is an employee of Pharmacyclics, USA and hold stocks in Pharmacyclics.

All authors met ICMJE criteria and all those who fulfilled those criteria are listed as authors. All authors had access to the study data and made the final decision about where to present these data.

Study was supported by funding from Janssen Research & Development, LLC, New Jersey, USA

This study is registered at ClinicalTrials.gov, NCT01674322

Figure legends:

Figure 1: Mean (SD) Logarithmic-Linear Ibrutinib (A) and PCI-45227 (B) Concentration-Time Profiles in Plasma and Whole Blood

Figure 2: Mean (SD) Ibrutinib and PCI-45227 Concentration- and Total Radioactivity - Time Profiles in Blood (A) and Plasma (B)

Figure 3A: Mean (SD) Cumulative Excretion Of Total Radioactivity In Urine And Feces

Figure 3B: Representative radio-chromatograms for human faeces after a single dose of 140 mg ^{14}C-ibrutinib; pool of the stools collected at 6 and 10 h post-dose (B1) and pools of the stools collected at 23, 36 and 53 h post-dose (B2) of a study participant

Figure 3C: Representative radio-chromatogram for human urine after a single dose of 140 mg 14C-ibrutinib

Figure 3D: Radio-chromatogram plasma – off line counting – representative sample at 1h post dose

Figure 4: Proposed metabolic scheme

Figure 5: Mass Balance bar graph showing UD (parent drug) and metabolite abundance in feces and urine expressed as % of the dose.

DMD Fast Forward. Published on December 8, 2014 as DOI: 10.1124/dmd.114.060061
This article has not been copyedited and formatted. The final version may differ from this version.

Table 1: Mean (SD) Pharmacokinetic Parameters and Total Radioactivity of Ibrutinib and PCI-45227

Parameter	Ibrutinib		PCI-45227		Total Radioactivity	
	Blood	**Plasma**	**Blood**	**Plasma**	**Blood**	**Plasma**
C_{max} (ng/mL)	33.9 (19.1)	37.1 (22.4)	49.6 (9.3)	43.5 (9.01)	480 (72.5)[b]	634 (87.9)[b]
T_{max} (h)[a]	0.52 (0.50 – 1.50)	0.52 (0.50 – 1.50)	0.78 (0.50 – 1.50)	0.78 (0.50 – 1.50)	0.78 (0.50 – 1.50)	0.77 (0.50 – 1.50)
T_{last} (h)	17.34 (3.26)	17.34 (3.26)	56.01 (12.39)	56.01 (12.39)	11.34 (6.89)	72.03 (0.03)
AUC_{24} (ng.h/mL)	NA	NA	248 (50.3)	227 (56.0)	NA	3690 (434)[c]
AUC_{last} (ng.h/mL)	52.0 (32.9)	61.5 (39.2)	280 (55.0)	257 (61.5)	1932 (1054)[c]	6821 (908)[c]
AUC_{∞} (ng.h/mL)	59.6 (31.6)	70.5 (37.8)	283 (54.7)	259 (60.7)	- -	- -
$t_{1/2}$ (h)	3.33 (0.98)	3.14 (0.81)	8.45 (0.84)	8.37 (0.88)	25.79 (35.93)	47.25 (11.60)
Vd/F (L)	14385 (9102)	11038 (5485)			708 (154)	941 (161)
CL/F (L/h)	2825 (1258)	2443 (1188)			46.3 (38.7)	14.2 (2.49)

CL_R (L/h)	0.00365
	(0.00156)

[a] Median (range); [b] ng.eq/mL; [c] ng.eq.h/mL; NA=not applicable

$AUC_{24,}$ area under the concentration-time curve from time 0 to 24 hours; $AUC_{last,}$ area under the concentration-time curve from time 0 to time of the last quantifiable concentration; AUC_{∞}, area under the concentration-time curve from time 0 to infinite time; $t_{1/2}$ elimination half-life; C_{max}, maximum concentration; CL/F, total clearance of drug after extravascular administration; CL_R, renal clearance of drug; t_{max}, time to reach the maximum concentration; t_{last}, time to last quantifiable concentration; Vd/F, apparent volume of distribution based on the terminal phase;

Table 2: Identification of in vivo metabolites of ibrutinib

Component	Identity	Retention time	m/z	m/z ^{14}C	Typical MS fragments	Matrix
M1	+138 (JNJ-54243696+O+Gluc)	10.21	579.2203	-	202-320-403-496	P
M4	+42 (JNJ-54243696+O+SO3)	12.81	483.1451	-	308-320-400-403-404	B,P
M7	+114 (N-ring opened alcohol+O+SO3)	14.24	555.1662	557.1694	156-320-404-457-475	U
M10	+130 (dihydrodiol+O+SO3)	15.75	571.1611	573.1643	154-172-320-403-431-461-473-491	U
M11	+48 (N-ringopened acid+O)	15.83	489.1886	491.1918	152-170-320-417-471	F,B,P
M17	+34 (N-ringopened alcohol+O)	17.64	475.2094	477.2126	138-156-320-404	F,U
M20	+48 (N-ringopened acid+O)	19.39	489.1886	491.1918	400-418	F,U,B,P
M21	+96 (+O+SO3)	19.57	537.1556	539.1588	84-138-320-403-457	U,B,P
M23	-54 (JNJ-54243696)	20.10	387.1933	-	84-181-209-287-304	F, B, P
M24	+52 (N-ring opened alcohol+2O+2H)	20.32	493.2199	495.2231	172-190-304-405-475	F,U,B,P
M25	+32 (N-ring opened acid)	20.89	473.1937	475.1969	152-170-304-342-401-455	F,U,B,P
M29	+34 (N-ring opened alcohol+O)	22.37	475.2094	477.2126	156-304-320-386-404	F,U,B,P
M30	(JNJ-54243696+O-2H)	22.79	401.1726	-	181-210-287-304	F, B, P
M31	+178 (+2H+CGSC)	23.10	619.2451	621.2549	304-387-441-473-601	B,P
M32	+163 (+2H+MASC)	23.71	604.2342	606.2374	304-387-441-473-562	F,U
M33	+161 (+MASC)	24.11	602.2186	604.2218	304-385-439-473	F
M34	+18, N-ring openedalcohol	23.63	459.2145	461.2177	84-102-138-156-304-321-388-441	F,U,B,P
M35	+16 (+O)	23.77	457.1988	459.2020	84-138-304-320-374-403	F,B
M36	+18 (+O+2H)	24.59	459.2145	461.2177	84-140+320+403	F
M37	+34 (dihydrodiol)	25.41	475.2094	477.2126	84-154-172-304-387-445-457	F,U,B,P
M39	+16 (+O)	28.06	457.1988	459.2020	304-385-439	B,P
M40	+16 (+O)	28.75	457.1988	459.2020	304-385-439	B,P
UD	Parent	30.20	441.2039	443.2071	304-385-439	F,B,P

Abbreviations: U: urine; F: feces B: blood; P: plasma SO3; sulfate conjugate; CGSC: cysteine-glycine conjugate; MASC: mercapturic acid conjugate; Gluc: glucuronide

DMD Fast Forward. Published on December 8, 2014 as DOI: 10.1124/dmd.114.060061
This article has not been copyedited and formatted. The final version may differ from this version.

Table 3: The levels of covalently bound radioactivity in plasma

Time (h)	Covalently bound radioactivity (ng eq./mL)	Total Radioactivity (ng eq./mL)
	Plasma pellet	Plasma
0	-	LOQ
0.5	-	520
1	47	549
1.5	-	447
2	55	364
3	-	259
4	48	195
6	-	141
8	65	135
12	-	115
16	-	98
24	61	94
48	-	60
72	25	47
C_{max}	65	549
C_{max} % of TR	12	100
T_{max}	8	1
AUC_{0-72h}	3488	6820
AUC_{0-72h} % of	51	100

TR		
AUC_{0-24h}	1414	3690
AUC_{0-24h} % of TR	38	100

LOQ: 36 ng eq./mL

C_{max}, maximum concentration; t_{max}, time to reach the maximum concentration; AUC_{0-24h}, area under the concentration-time curve from time 0 to 24 hours; AUC_{0-72h}, area under the concentration-time curve from time 0 to 72h; TR, total radioactivity; LOQ, limit of quantification

Figure 1:

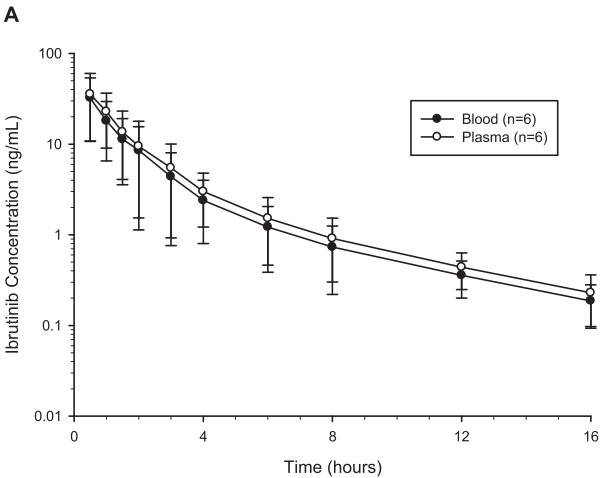
A
Ibrutinib Concentration (ng/mL)
100
10
1
0.1
0.01
0
4
8
12
16
Time (hours)
Blood (n=6)
Plasma (n=6)

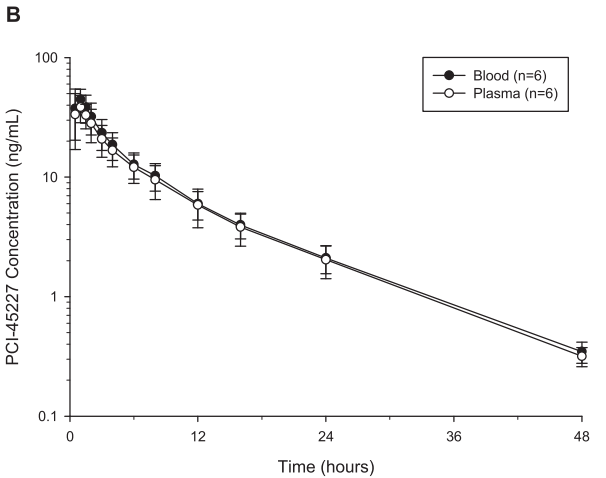
B
PCI-45227 Concentration (ng/mL)
100
10
1
0.1
0
12
24
36
48
Time (hours)
Blood (n=6)
Plasma (n=6)

Figure 2:

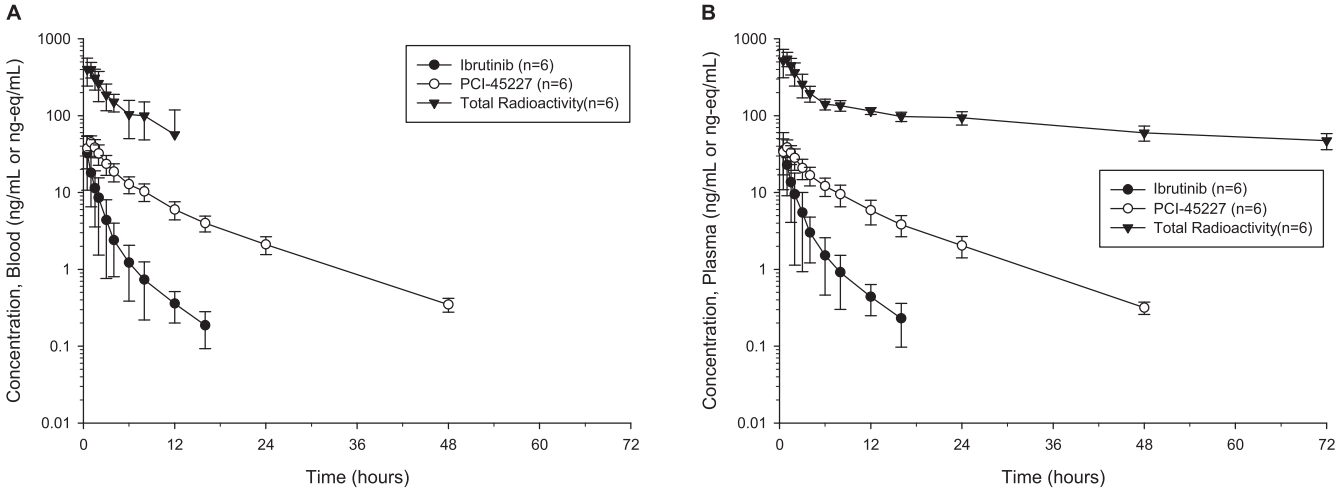
A
Concentration, Blood (ng/mL or ng-eq/mL)
1000
100
10
1
0.1
0.01
0
12
24
36
48
60
72
Time (hours)
Ibrutinib (n=6)
PCI-45227 (n=6)
Total Radioactivity(n=6)
B
Concentration, Plasma (ng/mL or ng-eq/mL)
1000
100
10
1
0.1
0.01
0
12
24
36
48
60
72
Time (hours)
Ibrutinib (n=6)
PCI-45227 (n=6)
Total Radioactivity(n=6)

Figure 3:

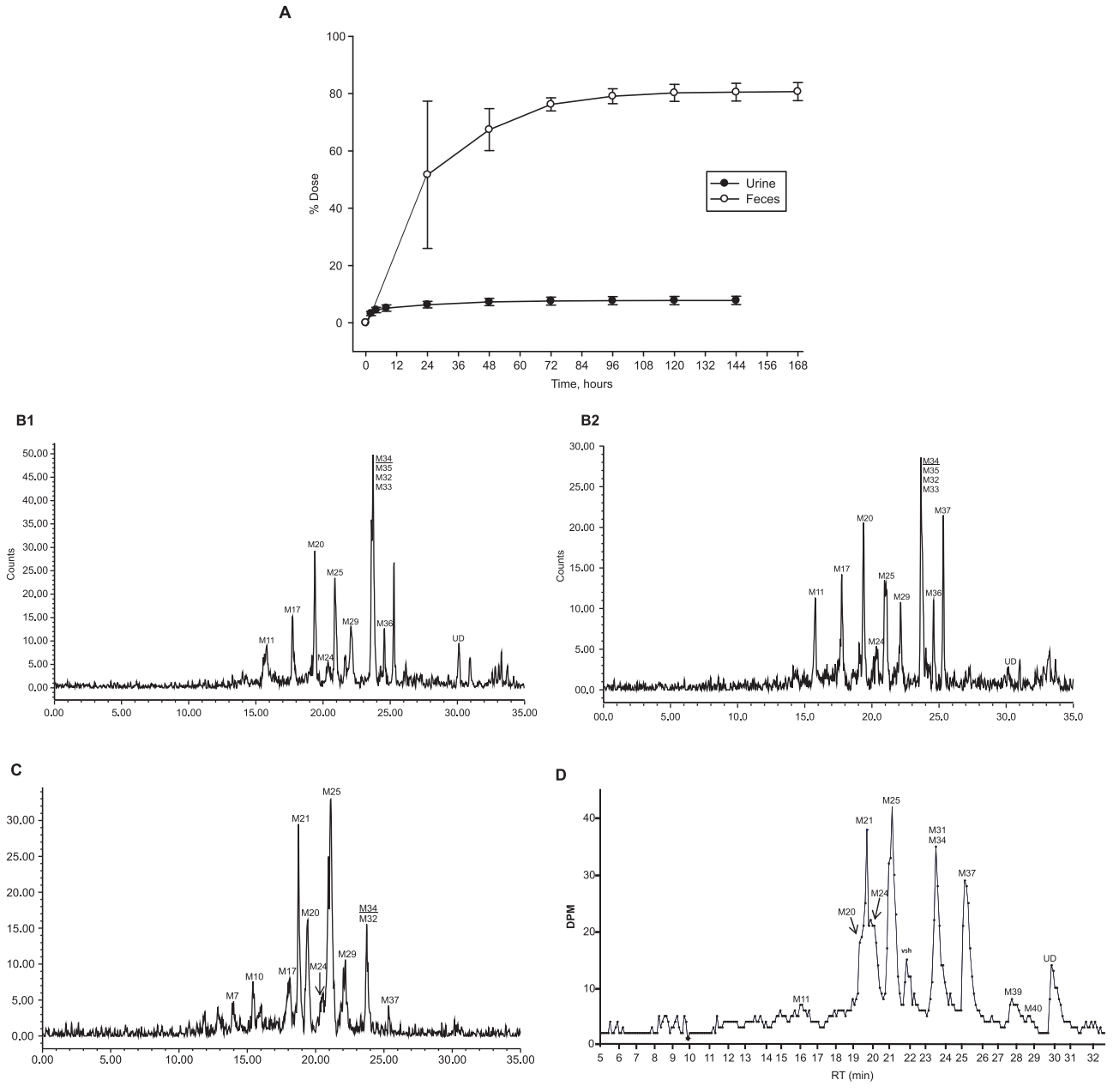
A
% Dose
Time, hours
Urine
Feces
B1
Counts
M11
M17
M20
M24
M25
M29
M34
M35
M32
M33
M36
UD
B2
Counts
M11
M17
M20
M24
M25
M29
M34
M35
M32
M33
M36
M37
UD
C
M7
M10
M17
M20
M21
M24
M25
M29
M34
M32
M37
D
DPM
RT (min)
M11
M20
M21
M24
M25
vsh
M31
M34
M37
M39
M40
UD

Figure 4:

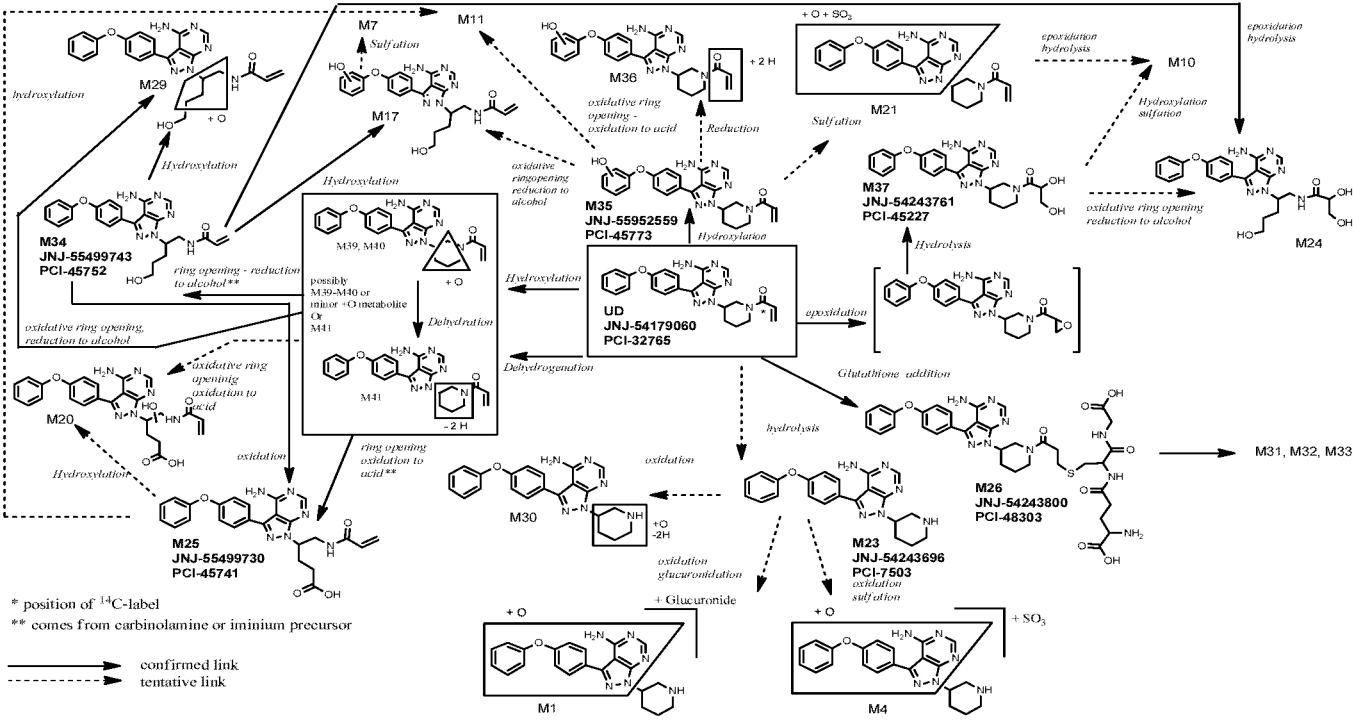

Note: In some instances the links between specific metabolites was established by *in vitro* incubation of the metabolic precursor

Figure 5:

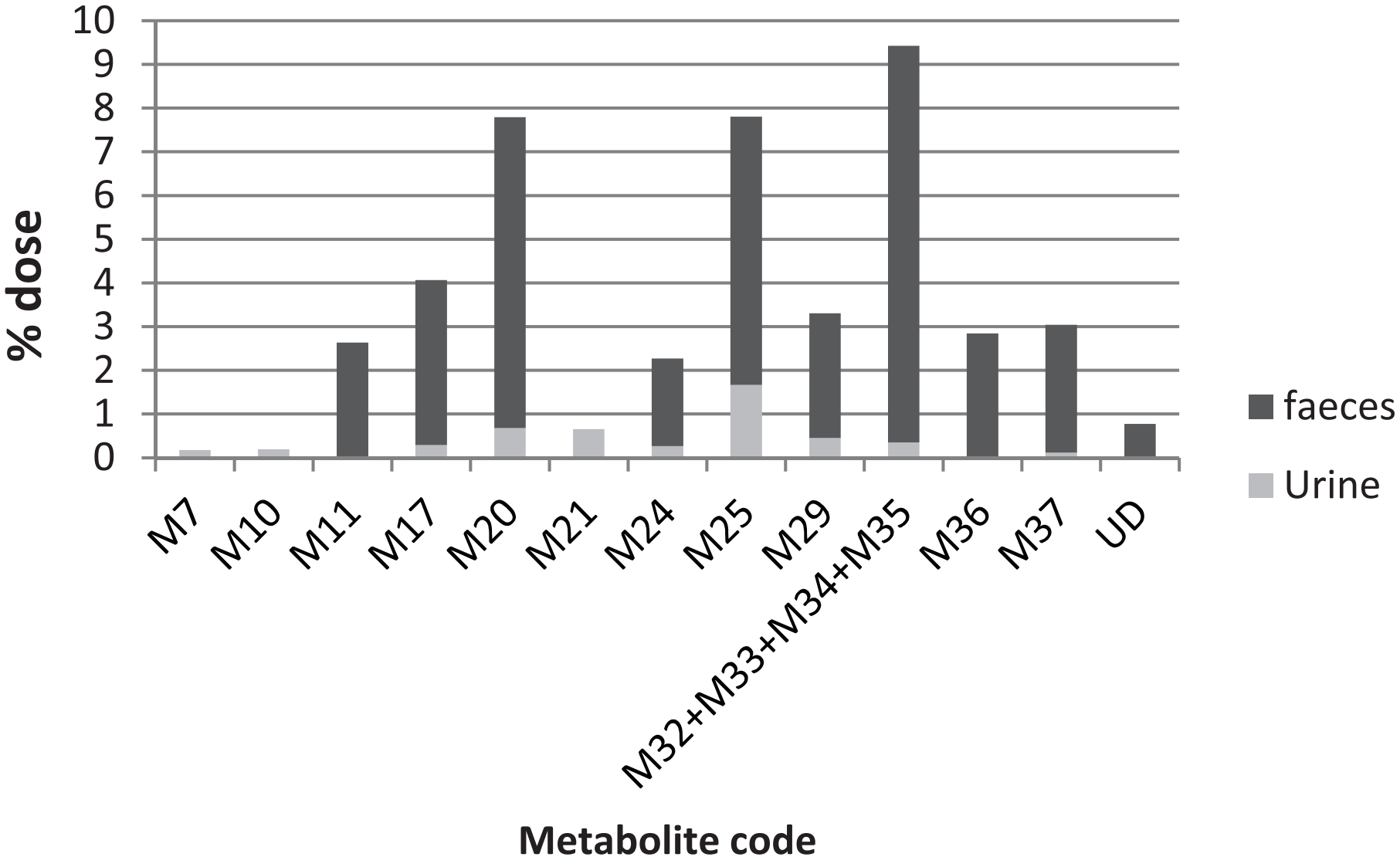
% dose
10
9
8
7
6
5
4
3
2
1
0
M7
M10
M11
M17
M20
M21
M24
M25
M29
M32+M33+M34+M35
M36
M37
UD
faeces
Urine
Metabolite code

Supplemental Data 1

TITLE:

Absorption, metabolism and excretion of oral ^{14}C radiolabeled ibrutinib: An open-label, phase I, single-dose study in healthy male participants

Authors:

Ellen Scheers[1], Laurent Leclercq[1], Jan de Jong[2], Nini Bode[3], Marc Bockx[1], Filip Cuyckens [1], Donna Skee[4], Joe Murphy[4], Juthamas Sukbuntherng[5], Geert Mannens[1]

[1]Pharmacokinetics, Dynamics and Metabolism, Janssen R&D, Beerse, Belgium;

[2]Clinical Pharmacology, Janssen R&D, San Diego, CA, USA;

[3]Pre-Clinical Project Development, Janssen R&D, Beerse, Belgium;

[4]Clinical Pharmacology, Janssen R&D, Raritan, NJ, US;

[5]Pharmacyclics, Sunnyvale, CA, USA;

Journal title: Drug Metabolism and Disposition

UPLC (Ultra Performance Liquid Chromatography) for metabolite profiling

Equipment:

- **Ultra Performance Liquid Chromatography:**

  Acquity Binary Solvent Manager / Waters 2777 CTC-Pal-injector

- **UV detector:**

  Acquity PDA

- **CDS System:**

  Empower 2

- **Online Radioactivity Detector:**

  Scintillation solvent : Ultima-Flo-M (14C-label), 3.8 mL/min using switching valve

- **MS Detector:**

  Waters QTof-Ultima

- **MS Data System:**

  Masslynx 4.1

Operating conditions:

- **Columns:**

  Interchim Uptisphere Strategy 100Å C18-2, 2.2 μm, 2 x (150 mm x 3.0 mm(id))

- **Column temperature:**

  T = 60°C

- **Mobile phase:**

  Solvent A: 0.025M Ammonium Acetate pH 5.0

  Solvent B: 20 / 80 (Methanol / Acetonitrile)

- **Elution mode:**

linear gradient:

time (min.)	0	30	31	34	35	40
% A	95	40	5	5	95	95
% B	5	60	95	95	5	5

- **Run Time:** 40 minutes
- **Flow:** 0.8 mL/min
- **Detector wavelength:** 285 nm

Calibration

The amount of unchanged drug and its respective metabolites was calculated from the radioactivity peaks. Areas of the radioactivity peaks, as computed by Empower 2 software, were converted into amount (of radioactivity) of ^{14}C-ibrutinib by the CDS system after introduction of a calibration curve [amount (of radioactivity) *versus* area of radioactivity peak] and linear regression analysis. A calibration curve was made up by 300 µL injections of known amounts of ^{14}C-ibrutinib (1158-78816 dpm) and was characterized by the following equation: $y = 0.992x - 1.13$ (with $r^2 = 0.995$).

QTOF settings for metabolite identification

The mass spectrometer (QTOF Ultima, Waters) was equipped with a dual electrospray ionisation probe and was operated in positive, in V- or W-mode. The capillary voltage was set at 3 kV and the cone at 40. The source temperature was 100°C, desolvation temperature 250°C. The mass spectrometer was calibrated with a Sodium Formate solution delivered through the Sample Spray. The LockSpray^{TM} ESI probe provided an independent source of the lock mass calibrant

Leucine Enkephaline. The Leucine ion at *m/z* 556.2771 was used as lock mass in full MS as well as in MSMS-mode. QTof data (MS, MSMS) were acquired in the centroid mode with a variable scantime (0.5 – 1.0 sec). All data were processed using the Masslynx software.

Supplemental Data 2

Table: Demographic and Baseline Characteristics

Participant	Sex	Age	Wght (kg)	Height (cm)	BMI (kg/m^2)	CLcr (mL/min)	2D6 genotype	2D6 gene activity	2D6 phenotype
1	Male	42	86.5	173	28.9	122	*5/*5	none/none	PM
2	Male	53	87.3	179	27.2	123	*4/*4	none/none	PM
3	Male	49	65.7	170	22.7	89.6	*1/*4	normal/none	EM
4	Male	55	81	179	25.3	109	*1/*1	normal/normal	EM
5	Male	35	61.7	163	23.2	131	*2/*41	none/reduced	EM
6	Male	53	84	179	26.2	127	*1/*4	norm/none	EM

CLcr, Creatinine clearance; EM, Extensive metabolizers; PM, Poor metabolizers